

A Maximum Stellar Surface Density in Dense Stellar Systems

Philip F. Hopkins,^{*}¹ Norman Murray,^{2,3} Eliot Quataert,¹ & Todd A. Thompson^{4,5,6}

¹*Department of Astronomy and Theoretical Astrophysics Center, University of California Berkeley, Berkeley, CA 94720*

²*Canadian Institute for Theoretical Astrophysics, 60 St. George Street, University of Toronto, ON M5S 3H8, Canada*

³*Canada Research Chair in Astrophysics*

⁴*Department of Astronomy, The Ohio State University, 140 W. 18th Ave., Columbus, OH 43210*

⁵*Center for Cosmology & Astro-Particle Physics, The Ohio State University, 191 W. Woodruff Ave., Columbus, OH 43210*

⁶*Alfred P. Sloan Fellow*

Submitted to MNRAS, August 10, 2009

ABSTRACT

We compile observations of the surface mass density profiles of dense stellar systems, including globular clusters in the Milky Way and nearby galaxies, massive star clusters in nearby starbursts, nuclear star clusters in dwarf spheroidals and late-type disks, ultra-compact dwarfs, and galaxy spheroids spanning the range from low-mass, “cusp” bulges and ellipticals to massive “core” ellipticals. We show that in all cases the maximum stellar surface density attained in the central regions of these systems is similar, $\Sigma_{\max} \sim 10^{11} M_{\odot} \text{ kpc}^{-2}$ ($\sim 20 \text{ g cm}^{-2}$), despite the fact that the systems span ~ 7 orders of magnitude in total stellar mass M_* , ~ 5 in effective radius R_e , and have a wide range in *effective* surface density M_*/R_e^2 . The surface density limit is reached on a wide variety of physical scales in different systems and is thus not a limit on three-dimensional stellar density. Given the very different formation mechanisms involved in these different classes of objects, we argue that a single piece of physics likely determines Σ_{\max} . The radiation fields and winds produced by massive stars can have a significant influence on the formation of both star clusters and galaxies, while neither supernovae nor black hole accretion are important in star cluster formation. We thus conclude that feedback from massive stars likely accounts for the observed Σ_{\max} , plausibly because star formation reaches an Eddington-like flux that regulates the growth of these diverse systems. This suggests that current models of galaxy formation, which focus on feedback from supernovae and active galactic nuclei, are missing a crucial ingredient.

Key words: galaxies: formation — galaxies: evolution — galaxies: active — star formation: general — cosmology: theory

1 INTRODUCTION

Feedback from massive stars and black holes is widely believed to play a critical role in the formation of other stars, stellar clusters, and entire galaxies. However, the precise physical mechanism(s) that dominate the coupling between stars and/or black holes and their surrounding environment have not been definitively established. Unlike the energy deposited by, e.g., a jet, the momentum produced by a central star or accreting black hole cannot be radiated away. When the momentum deposition rate exceeds the strength of gravity, gas can be efficiently expelled from the system. This limit is analogous to the Eddington limit from stellar physics; however, the gas in star-forming regions and galaxies is dusty, and thus the appropriate opacity is not that of electron scattering, but

the much larger opacity due to dust (see e.g. Scoville et al. 2001; Murray et al. 2005; Thompson et al. 2005).

This generalization of the Eddington limit has been posited as an explanation for the characteristic sizes of massive stellar clusters (Murray 2009), as well as the maximum luminosities of the most rapidly star-forming objects in the Universe, bright sub-millimeter galaxies with $\sim 10^{13} L_{\odot}$ inside of $\sim \text{kpc}$ (star formation rates $\gtrsim 1000 M_{\odot} \text{ yr}^{-1} \text{ kpc}^{-2}$; e.g., Younger et al. 2008; Walter et al. 2009). Outflows driven by radiation pressure may help explain phenomena as diverse as turbulence in star-forming regions, the relation between galaxy mass and stellar population metallicity, the correlations between the masses of black holes and their host spheroids, and the abundance patterns of the IGM (see e.g. Murray et al. 2005; Thompson et al. 2005; Oppenheimer & Davé 2006, 2008; Krumholz et al. 2009; Murray et al. 2009; Krumholz & Matzner 2009). Small changes in the nature of stellar feedback — for example, whether or not winds are really momentum or pressure

* E-mail: phopkins@astro.berkeley.edu

driven, or the characteristic scales of wind driving — have dramatic consequences for predictions of models of galaxy formation, affecting the global structure of even Milky Way-mass systems (Governato et al. 2007; Scannapieco et al. 2008).

Outflows appear to be ubiquitous from rapidly star-forming galaxies (Heckman et al. 1990; Martin 1999, 2005; Heckman et al. 2000; Erb et al. 2006; Weiner et al. 2009). However, quantifying the basic properties of these outflows is challenging; their mass-loading, dynamical importance, and implications for future star formation remain subjects of considerable debate. This uncertainty translates into uncertainty in the dominant physical processes driving such outflows (e.g., radiation pressure, supernovae, AGN vs. star formation, etc.). It is also unclear whether or not feedback processes and the outflows they generate actually leave an imprint on the structural properties of star clusters and galaxies.

In this *Letter*, we show that a diverse set of dense stellar systems — from star clusters to the centers of elliptical galaxies — have a maximum stellar surface density. We argue that this observational fact provides a strong constraint on models of feedback in star cluster and galaxy formation, pointing to the critical role of massive stars, rather than supernovae or AGN. In § 2, we present our compilation of observations of dense stellar systems (Table 1), and compare their surface density profiles and maximum surface densities. In § 3, we discuss the implications of our results and interpret the observed maximum stellar surface density in terms of models in which star formation reaches the (dust) Eddington limit.

Throughout, we adopt a $\Omega_M = 0.3$, $\Omega_\Lambda = 0.7$, $h = 0.7$ cosmology and a Chabrier (2003) stellar IMF, but these choices do not affect our conclusions. Changes in the IMF would systematically shift the stellar masses of the massive systems, but reasonable (factor < 2) changes are within the scatter in the data we compile.

2 OBSERVATIONAL RESULTS

In Table 1, we summarize our compilation of a large sample of the observed surface density profiles of dense stellar systems, including globular clusters (GCs) in the Milky Way and nearby galaxies,¹ the nuclear stellar disk observed around Sgr A* in the galactic center, massive star clusters in starburst regions, nuclear star clusters in dwarf spheroidals and late-type disks, ultra-compact dwarfs, and classical spheroidals spanning the range from low-mass, “cusp” bulges and ellipticals (those with steep central surface brightness slopes) to massive “core” galaxies (these predominate at the highest masses, with shallower central slopes). We also include massive compact ellipticals observed at high redshifts, $z \sim 2 - 3$; as already shown in Hopkins et al. (2009a) and Bezanson et al. (2009), these compact high z systems in fact have the same maximum density as the central regions of today’s ellipticals.

For each object, we adopt the best-fit surface brightness profile determined by the authors. This is usually a King (1966) profile for the less massive systems, and a Sersic (1968) or Nuker profile for the more massive objects. For the MW nuclear stellar disk we adopt the total mass from Lu et al. (2009) and the profile shape fitted in Paumard et al. (2006) ($\Sigma \propto (R^2 + R_{\text{core}}^2)^{-1}$). The data from Kormendy et al. (2009) and Lauer et al. (2007) span sufficient dynamic range that we directly adopt the observed (PSF de-convolved) profiles rather than a fit to the data; for the other systems in Table 1, the data do not span sufficient dynamic range to see significant deviations from the fits used here. In all cases,

¹ We do not distinguish between GCs that might have undergone core collapse and those that have not.

Table 1. Observations of Dense Stellar Systems

Reference ¹	Description ²	Symbol ³
Lu et al. (2009)	MW Nuclear Disk	dark green square
Harris (1996)	MW GCs	pink circle
Barmby et al. (2007)	M31 GCs	yellow circle
Rejkuba et al. (2007)	Massive Cen A GCs	green pentagon
McCraday & Graham (2007)	M82 SSCs	orange ×
Walcher et al. (2005)	Sd+dSph nuclear SCs	red +
Böker et al. (2004)	Sd disk nuclear SCs	magenta asterisk
Geha et al. (2002)	dSph nuclei	violent inv. triangle
Haşegan et al. (2005)	M87 UCDs	light blue star
Evstigneeva et al. (2007)	Virgo UCDs	dark blue triangle
Hilker et al. (2007)	Fornax UCDs	cyan diamond
Kormendy et al. (2009)	Virgo Es	red circle
Lauer et al. (2007)	local massive Es	violet square
van Dokkum et al. (2008)	$z = 2 - 3$ massive Es	orange star

¹For most of the objects we adopt the fitted functional forms for the density profiles presented in each paper. For the Kormendy et al. (2009) and Lauer et al. (2007) samples, however, the data are sufficiently high dynamic range that we use the observed profiles directly. Note that the profiles shown in Lauer et al. (2007) include only the HST data; the profiles used here are the composite (HST+ground-based) profiles used therein to determine effective radii.

²GC=Globular cluster, SC=Star cluster, SSC=Super star cluster, UCD=Ultra-compact dwarf, E=elliptical. Note that Geha et al. (2002) and Walcher et al. (2005) refer to their dwarf galaxy hosts of nuclear star clusters as dEs; we follow Kormendy et al. (2009) and classify these as dwarf spheroidals (dSph).

³Plotting symbol used for objects in each sample throughout.

we convert the measured light profiles to stellar mass density profiles by first adopting the authors’ determination of total stellar masses (re-normalized to our Chabrier 2003 IMF where appropriate). We then assume a radius-independent stellar mass-to-light ratio to convert the light profiles to mass profiles. The assumption of a radius-independent M_*/L is reasonable for the well-resolved galactic systems (nuclear SCs and Es), which are relatively old and have weak observed color or stellar population gradients (see e.g. Côté et al. 2006; Sánchez-Blázquez et al. 2007; Hopkins et al. 2008). The lower-mass systems (e.g. GCs) are approximately single stellar populations, so this should be a reasonable first approximation in those cases as well. In the high z ellipticals the central densities are unresolved; we thus extrapolate the best-fit Sersic profiles inwards. For low-redshift ellipticals, this extrapolation is typically a factor ~ 2 higher than the true central densities (see Hopkins et al. 2009a for more details).

The left panel of Figure 1 shows the *effective* surface mass densities $M_*/\pi R_e^2$ of these dense stellar systems as a function of their total stellar mass, where R_e is the projected half-stellar mass radius. The wide range of systems shown in Figure 1 differ significantly in their large-scale structure and formation mechanisms. Various works have compared these different object classes in this and other projections of the fundamental plane, e.g., in the space of effective surface or luminosity density, mass, mass-to-light ratio, size, or velocity dispersion (Kormendy 1985; Geha et al. 2002; Haşegan et al. 2005; Rejkuba et al. 2007; Evstigneeva et al. 2007; Dabringhausen et al. 2008; Hopkins et al. 2009b). In some of these correlations there is apparent continuity from star clusters to massive galaxies, but in others, different objects trace nearly perpendicular correlations and thus appear physically quite distinct. In terms of their effective densities, Figure 1 shows that massive galaxies are significantly less dense than low-mass stellar clusters, and there is no indication of a universal maximum stellar surface density.

However, Σ is of course higher at small $R \ll R_e$. Figure 2 thus directly compares the surface mass density profiles of these different systems. For clarity, rather than plotting every individual

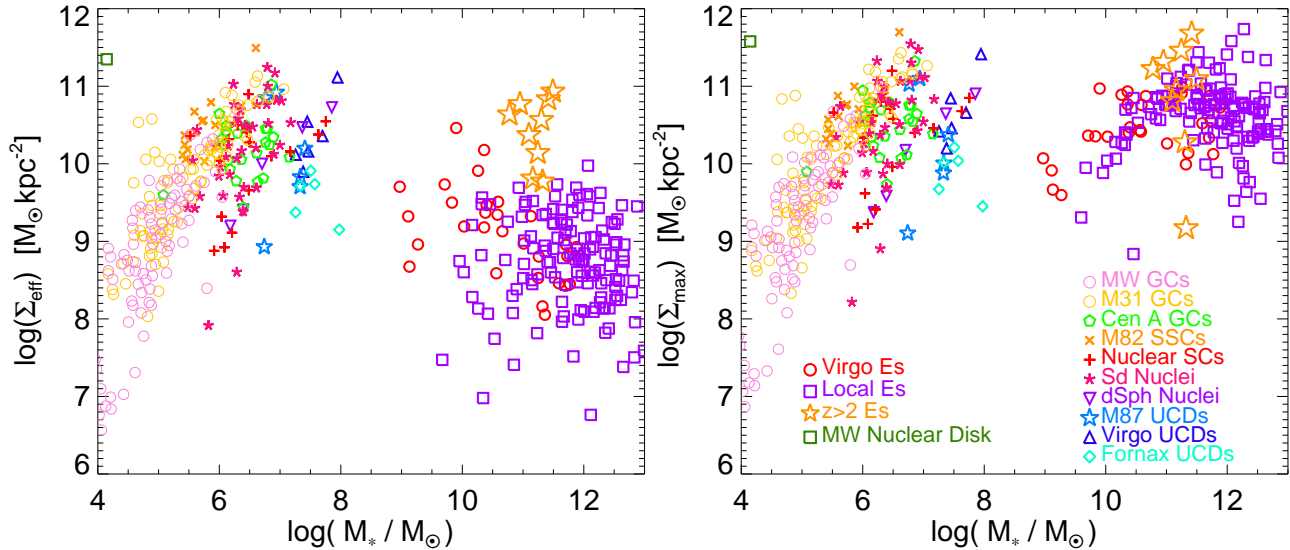


Figure 1. *Left:* Effective surface mass density $\Sigma_{\text{eff}} \equiv M_*(< R_e) / \pi R_e^2$ as a function of total stellar mass for the different samples described in the text and legend. *Right:* Maximum surface mass density Σ_{max} obtained at small radii in the surface brightness profile (see Fig. 2), as a function of total stellar mass, for the different samples described in the text and legend. The effective densities vary significantly across the different samples. However, there appears to be a well-defined upper limit $\sim 10^{11} M_{\odot} \text{ kpc}^{-2}$ to the maximum surface mass density; this limit holds for the full range of dense stellar systems considered here.

profile, we plot the median and $\pm 1\sigma$ scatter in $\Sigma(R)$ at each R for each class of objects listed in Table 1 (we neglect the low-mass GCs, which have much lower densities in Figure 1 and remain relatively low-density at all radii). Since the elliptical samples, in particular that of Kormendy et al. (2009), span a very large range in R_e and M_* , we split them into 3 classes: low-mass ellipticals in Virgo ($M_* < 10^{10} M_{\odot}$) and high mass cusp and core ellipticals.

Figure 2 shows that the surface density profiles appear to asymptote to a maximum $\Sigma_{\text{max}} \sim 10^{11} M_{\odot} \text{ kpc}^{-2} \sim 20 \text{ g cm}^{-2}$, independent of object class, despite spanning an enormous range of M_* and R_e . The most massive Es maintain this density out to few 100 pc scales, with Σ decreasing only weakly with radius. Massive GCs, on the other hand, also reach this surface density at small radii, but their densities then fall off rapidly with radius. Note that radii $\ll \text{pc}$ are not resolved and are thus not plotted for these systems; extrapolations of the King model fits to arbitrarily small R , however, do not significantly exceed the maximum densities shown in Figure 2. Even the MW nuclear disk, with its proximity to the nuclear black hole and evidence for a top-heavy IMF (Nayakshin & Sunyaev 2005), does not appear to exceed Σ_{max} . Interestingly, recent observations suggest that there is a nuclear star cluster in the center of the Milky Way. The observations favor a radius-independent stellar surface density $\approx 1.5 - 3 \times 10^{11} M_{\odot} \text{ kpc}^{-2}$ from $\sim 0.02 - 1.0 \text{ pc}$ (Schoedel et al. 2009); this is comparable to Σ_{max} found here.

The right panel of Figure 1 shows the *maximum* stellar surface density Σ_{max} of each object as a function of its total stellar mass. For the King profile objects, Σ_{max} is defined to be the surface density inside the fitted “core” radius ($\sim R_e$). For the ellipticals, we define Σ_{max} as the $\langle \Sigma \rangle$ inside the radius where Σ falls a factor ~ 2 below the maximum Σ measured. Reasonable variations in our definition of Σ_{max} make little difference to our general conclusion: although the effective densities of dense stellar systems (left panel) vary widely, many such systems (and most of the object classes) have roughly the same maximum stellar surface density $\sim 10^{11} M_{\odot} \text{ kpc}^{-2}$ at small radii, over a factor of $\sim 10^7$ in M_* .

3 DISCUSSION AND INTERPRETATION

The fact that a wide range of star clusters, dwarf galaxies, and massive galaxies have the same maximum stellar surface density $\Sigma_{\text{max}} \sim 10^{11} M_{\odot} \text{ kpc}^{-2} \sim 20 \text{ g cm}^{-2}$ suggests that a common physical process operated during the formation of these diverse systems to limit the stellar density that could be attained. It is worth emphasizing that the observed maximum is a maximum *surface* density. The different radii and masses sampled here imply that the same surface density corresponds to very different *three-dimensional* mass densities ρ . Whatever process regulates the growth of these systems selects a particular surface density, *not* a particular three-dimensional density.

It is, in principle, possible that the observed Σ_{max} is due to the absence of sufficient gas reaching surface densities $\gg \Sigma_{\text{max}}$. For example, in galaxy mergers, the high star formation efficiency in pre-merger disks with high gas fractions and masses, as well as the inefficient angular momentum loss during gas-rich mergers, mean that it is difficult to generate gas surface densities far in excess of Σ_{max} on scales $\gtrsim 100 \text{ pc}$ (see e.g. Hopkins et al. 2009c); this same conclusion may not, however, hold on smaller scales where Σ is nonetheless observed to be $\lesssim \Sigma_{\text{max}}$ (Fig. 2). In the case of star clusters, the masses of the most massive giant molecular cloud (GMC) complexes present a similar limitation; on $\sim 1 - 10 \text{ pc}$ scales, gas surface densities $\gg \Sigma_{\text{max}}$ would require GMC masses in excess of $\sim 10^7 - 10^8 M_{\odot}$, at the limit of those inferred observationally.

The observed maximum surface density occurs, however, over a huge dynamic range in mass ($\sim 10^6 - 10^{12} M_{\odot}$), effective radius ($\sim 3 \text{ pc} - 50 \text{ kpc}$), stellar population age (young clusters with ages $\sim 10^6 \text{ yr}$ to spheroids and globular clusters with ages $\gtrsim 10 \text{ Gyr}$) and other properties. The formation mechanisms and formation timescales of these different classes of objects are also very different. Whatever determines their maximum surface density cannot, therefore, be specific to details of their formation or their global properties (e.g., M_* , R_e , etc.). As a result, it requires significant fine-tuning for the same Σ_{max} to apply independently, due to the availability of gas, in such a wide range of systems. Instead, it

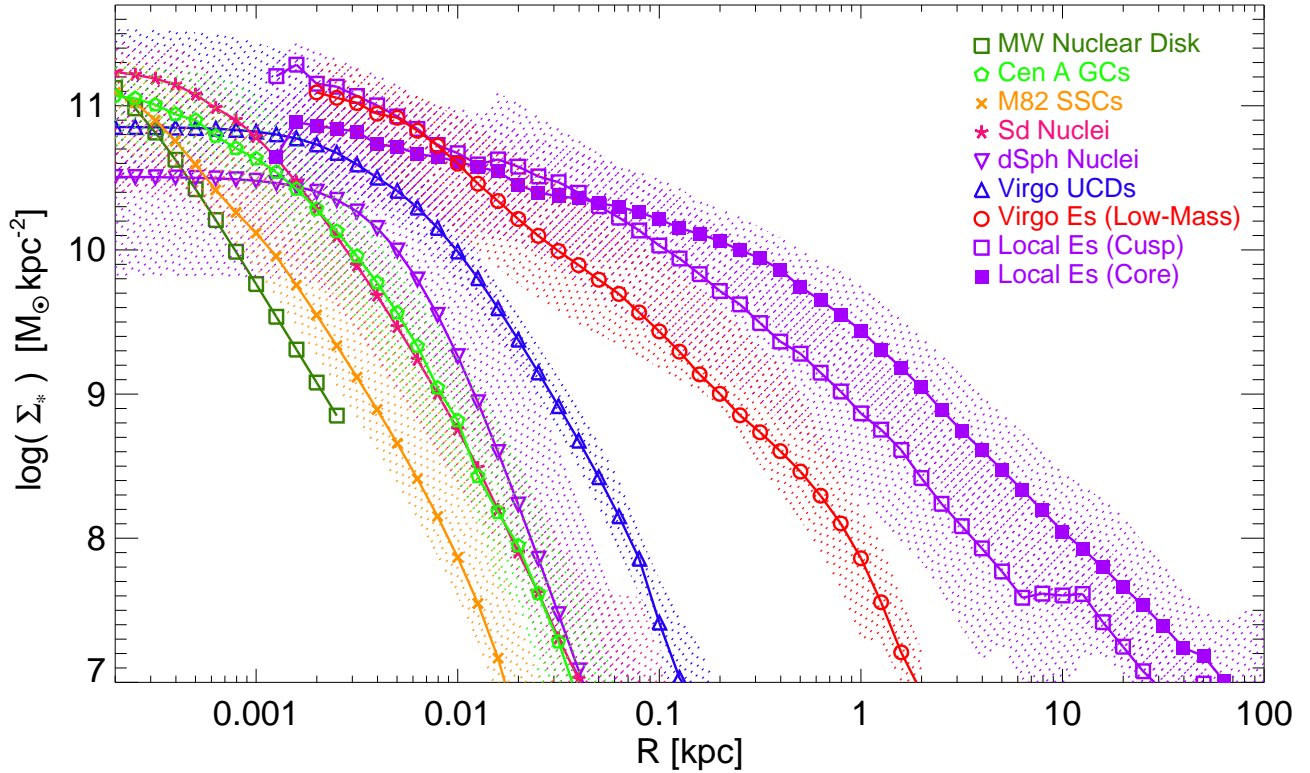


Figure 2. Stellar mass surface density profiles for the different samples. For each object class, thick solid lines (with points) show the median stellar mass surface density profile; shaded range shows the $\pm 1\sigma$ dispersion. The upper limit $\sim 10^{11} M_{\odot} \text{ kpc}^{-2}$ is apparent, across a variety of classes.

appears likely that there is some rather generic physics that sets Σ_{max} . The key traits the systems we consider share are that they are baryon-dominated and likely formed in dissipational (rapid, gas-dominated) events. Because star clusters form and disrupt on a timescale much less than the time for massive stars to explode as supernovae (e.g., Murray et al. 2009), and because the time for stars to form at $\Sigma \sim \Sigma_{\text{max}}$ is also less than the time for massive stars to explode,² it is unlikely that supernova feedback is important in setting Σ_{max} . Similarly, there is no evidence for energetically important black hole accretion during star cluster formation. The similarity of Σ_{max} in both star clusters and galaxies thus suggests that massive stars themselves (on or near the main sequence) are critical for setting the observed Σ_{max} in dense stellar systems. Although we do not have a fully satisfactory theoretical explanation for Σ_{max} in the context of this interpretation, we briefly describe the possibility that it is set when these systems reach the dust Eddington limit.

The Eddington luminosity (L_{Edd}) or flux (F_{Edd}) for dusty gas is

$$\frac{L_{\text{Edd}}}{M_{\text{tot}}} = \frac{F_{\text{Edd}}}{\Sigma_{\text{tot}}} = \frac{4\pi Gc}{\kappa_F} \approx 2500 \kappa_{10}^{-1} \text{ ergs s}^{-1} \text{ g}^{-1}, \quad (1)$$

where κ_{10} is the opacity in units of $10 \text{ cm}^2 \text{ g}^{-1}$, M_{tot} and Σ_{tot} are the total enclosed mass and surface density, and κ_F is the flux-mean dust opacity. When the medium is optically-thick to the re-radiated FIR emission ($\Sigma_g \gtrsim 0.5 \text{ cm}^2 \text{ g}^{-1}$) κ_F can be approximated by the Rosseland-mean dust opacity, which has the form $\kappa_R \approx \kappa_0 T^2$ for $T \lesssim 200 \text{ K}$ and $\kappa_R \sim 5 - 10 \text{ cm}^2 \text{ g}^{-1} \approx \text{constant}$ for $200 \text{ K} \lesssim T \lesssim T_{\text{sub}}$, where $\kappa_0 \approx 2 \times 10^{-4} \text{ cm}^2 \text{ g}^{-1} \text{ K}^{-2}$ and $T_{\text{sub}} \sim 1500 \text{ K}$ is the

² Note that the dynamical timescale is $t_{\text{dyn}} \sim (G\Sigma_{\text{max}}/r)^{-1/2} \sim 1.5 \times 10^5 r_{10}^{1/2} \text{ yr}$, where $r_{10} = r/10 \text{ pc}$.

sublimation temperature of dust (Semenov et al. 2003). The surface densities in Figures 1 & 2 are sufficiently high that if the systems had gas fractions of order $f_g \sim 0.01$ or larger during formation, then the medium was optically-thick in the FIR ($\kappa_R f_g \Sigma_{\text{max}} > 1$). For gas fractions of order unity, the temperature deep inside the optically thick gas was $T \gtrsim 200 \text{ K}$ and $\kappa_R \sim 5 - 10 \text{ cm}^2 \text{ g}^{-1}$ (for solar metallicity and Galactic gas-to-dust ratio). These considerations motivate our scaling for κ in the last equality of equation (1).

We can compare the Eddington flux to the flux from star formation implied by a given gas surface density if we extrapolate the observed Kennicutt-Schmidt relation. From Kennicutt (1998), $\dot{\Sigma}_* \approx 2.5 \times 10^{-4} M_{\odot} \text{ yr}^{-1} \text{ kpc}^{-2} [\Sigma_{\text{gas}}/M_{\odot} \text{ pc}^{-2}]^{1.5}$; other studies of high surface density systems suggest the index may be somewhat steeper, ~ 1.7 (Bouché et al. 2007). Together with the empirically calibrated relation between SFR and bolometric or total infrared luminosity, $L_{\text{SF}} = 2.22 \times 10^{36} \text{ W} (\dot{M}_*/M_{\odot} \text{ yr}^{-1})$, this yields a simple scaling of flux from young stars versus surface density;

$$\frac{F_{\text{SF}}}{\Sigma_{\text{gas}}} \approx 2.8 \text{ ergs s}^{-1} \text{ g}^{-1} \left(\frac{\Sigma_{\text{gas}}}{10^6 M_{\odot} \text{ kpc}^{-2}} \right)^{0.5-0.7} \quad (2)$$

This relation shows that the flux from star formation reaches and then exceeds the threshold set by equation (1) for $\Sigma_{\text{gas}} \sim 10^{11} - 10^{12} M_{\odot} \text{ kpc}^{-2}$ (depending on the index adopted), suggestively similar to the maximum we find. The Eddington flux can indeed be produced by a young stellar population ($\lesssim 10^{6.6} \text{ yr}$), for which the stellar light to mass ratio is $\Psi \equiv F_*/\Sigma_* \approx 3000 \text{ ergs s}^{-1} \text{ g}^{-1}$ for a standard IMF. A young stellar population is thus just capable of reaching the dust Eddington limit and supporting an optically-thick self-gravitating medium with radiation pressure. In this limit, however, it is unclear whether stellar radiation pressure can ac-

count for a maximum surface density Σ_{\max} since both $F_* \propto \Sigma_*$ and $F_{\text{edd}} \propto \Sigma_{\text{tot}}$.

Another possibility is that the relevant luminosity could, for a short period of time, come directly from the inflow of gas required to form the system, rather than from starlight. If a gas-dominated system of mass M and surface density Σ collapses on a free-fall time, the luminosity due to the release of gravitational binding energy is $L \simeq \dot{M} v_{\text{ff}}^2 \propto \Sigma^{5/4} M^{1/4}$, where $\dot{M} \simeq M/[R/v_{\text{ff}}]$ is the inflow rate and v_{ff} is the free-fall velocity. Comparing the inflow luminosity with the Eddington luminosity, it is straightforward to show that there is a critical surface density above which the inflow luminosity exceeds the Eddington luminosity: $\Sigma_{\text{crit}} \approx 3 \times 10^{11} M_{\odot} \text{kpc}^{-2} \kappa_{10}^{-4/5} M_8^{1/5}$, where $M_8 = M/10^8 M_{\odot}$ is the mass at $\Sigma \sim \Sigma_{\text{crit}}$, which is not necessarily equal to the total mass of the system. This estimate is intriguing both because it is close to our observationally-inferred maximum surface density and because it provides a clear mechanism for obtaining a *maximum* in the gas (and ultimately stellar) surface density: the flux produced by inflow $\propto \Sigma^{9/4}$ increases more rapidly with surface density than the Eddington flux $\propto \Sigma$ so the system would likely adjust to have $\Sigma \sim \Sigma_{\text{crit}}$. However, the required inflow rates are extremely large, $\dot{M} \sim 2000 M_8^{3/4} M_{\odot} \text{yr}^{-1}$ at $\Sigma \sim 10^{11} M_{\odot} \text{kpc}^{-2}$, and must be present even at very small radii ($\sim \text{pc}$ for star clusters and $\lesssim 10 - 100 \text{ pc}$ for massive galaxies). These required inflow luminosities are significantly larger than we have found in a preliminary analysis of our numerical simulations of the mergers of very massive gas-rich galaxies. As a result, it appears unlikely that the high inflow luminosities required to reach the dust Eddington luminosity can in fact be realized in all of the systems considered in Figure 2.

One concern about invoking the dust Eddington limit is that the GCs in Figures 1 & 2 have low metallicities, typically ~ 0.1 solar, but sometimes even lower. As a result the dust opacity will be ~ 10 times smaller than that used in equation (1) and the massive stars present during GC formation would not reach $\sim F_{\text{Edd}}$. We note, however, that the winds from massive stars have a momentum flux comparable to that of the photons (e.g., Leitherer et al. 1999) and could have an impact similar to that attributed to photons here.

The maximum surface density found here could readily be exceeded if gas “trickled in” slowly from large radii, and was allowed to form stars for a long time and at a low rate. In principle, there should be no limit to how large a stellar surface density might be attained in this case because all forms of feedback would be ineffective at low star formation rates; in particular, the system would remain well below the Eddington limit. The interpretation given here requires that the high-density portions of the galaxy or cluster form in no more than a few, rapid events; this appears consistent with other observational indicators (e.g. the stellar populations).

ACKNOWLEDGMENTS

We thank Tod Lauer and Kevin Bundy for helpful discussions and the Aspen Center for Physics, where a portion of this work was conceived. Support for PFH was provided by the Miller Institute for Basic Research in Science, University of California Berkeley. EQ is supported in part by NASA grant NNG06GI68G and the David and Lucile Packard Foundation. TAT is supported in part by an Alfred P. Sloan Fellowship.

REFERENCES

- Barmby, P., McLaughlin, D. E., Harris, W. E., Harris, G. L. H., & Forbes, D. A. 2007, *AJ*, 133, 2764
- Bezanson, R., van Dokkum, P. G., Tal, T., Marchesini, D., Kriek, M., Franx, M., & Coppi, P. 2009, *ApJ*, 697, 1290
- Böker, T., Sarzi, M., McLaughlin, D. E., van der Marel, R. P., Rix, H.-W., Ho, L. C., & Shields, J. C. 2004, *AJ*, 127, 105
- Bouché, N., et al. 2007, *ApJ*, 671, 303
- Chabrier, G. 2003, *PASP*, 115, 763
- Côté, P., et al. 2006, *ApJS*, 165, 57
- Dabringhausen, J., Hilker, M., & Kroupa, P. 2008, *MNRAS*, 386, 864
- Erb, D. K., Shapley, A. E., Pettini, M., Steidel, C. C., Reddy, N. A., & Adelberger, K. L. 2006, *ApJ*, 644, 813
- Evstigneeva, E. A., Gregg, M. D., Drinkwater, M. J., & Hilker, M. 2007, *AJ*, 133, 1722
- Geha, M., Guhathakurta, P., & van der Marel, R. P. 2002, *AJ*, 124, 3073
- Governato, F., Willman, B., Mayer, L., Brooks, A., Stinson, G., Valenzuela, O., Wadsley, J., & Quinn, T. 2007, *MNRAS*, 374, 1479
- Haşegan, M., et al. 2005, *ApJ*, 627, 203
- Harris, W. E. 1996, *AJ*, 112, 1487
- Heckman, T. M., Armus, L., & Miley, G. K. 1990, *ApJS*, 74, 833
- Heckman, T. M., Lehnert, M. D., Strickland, D. K., & Armus, L. 2000, *ApJS*, 129, 493
- Hilker, M., Baumgardt, H., Infante, L., Drinkwater, M., Evstigneeva, E., & Gregg, M. 2007, *A&A*, 463, 119
- Hopkins, P. F., Bundy, K., Murray, N., Quataert, E., Lauer, T., & Ma, C.-P. 2009a, *MNRAS*, accepted, arXiv:0903.2479 [astro-ph]
- Hopkins, P. F., Cox, T. J., Dutta, S. N., Hernquist, L., Kormendy, J., & Lauer, T. R. 2009b, *ApJS*, 181, 135
- Hopkins, P. F., Cox, T. J., & Hernquist, L. 2008, *ApJ*, 689, 17
- Hopkins, P. F., Cox, T. J., Younger, J. D., & Hernquist, L. 2009c, *ApJ*, 691, 1168
- Kennicutt, Jr., R. C. 1998, *ApJ*, 498, 541
- King, I. R. 1966, *AJ*, 71, 64
- Kormendy, J. 1985, *ApJ*, 295, 73
- Kormendy, J., Fisher, D. B., Cornell, M. E., & Bender, R. 2009, *ApJS*, 182, 216
- Krumholz, M. R., Klein, R. I., McKee, C. F., Offner, S. S. R., & Cunningham, A. J. 2009, *Science*, 323, 754
- Krumholz, M. R., & Matzner, C. D. 2009, *ApJ*, in press, arXiv:0906.4343
- Lauer, T. R., et al. 2007, *ApJ*, 664, 226
- Leitherer, C., et al. 1999, *ApJS*, 123, 3
- Lu, J. R., Ghez, A. M., Hornstein, S. D., Morris, M. R., Becklin, E. E., & Matthews, K. 2009, *ApJ*, 690, 1463
- Martin, C. L. 1999, *ApJ*, 513, 156
- . 2005, *ApJ*, 621, 227
- McCraday, N., & Graham, J. R. 2007, *ApJ*, 663, 844
- Murray, N. 2009, *ApJ*, 691, 946
- Murray, N., Quataert, E., & Thompson, T. A. 2005, *ApJ*, 618, 569
- . 2009, *ApJ*, in press [arXiv:0906.5358]
- Nayakshin, S., & Sunyaev, R. 2005, *MNRAS*, 364, L23
- Oppenheimer, B. D., & Davé, R. 2006, *MNRAS*, 373, 1265
- . 2008, *MNRAS*, 387, 577
- Paumard, T., et al. 2006, *ApJ*, 643, 1011
- Rejkuba, M., Dubath, P., Minniti, D., & Meylan, G. 2007, *A&A*, 469, 147
- Sánchez-Blázquez, P., Forbes, D. A., Strader, J., Brodie, J., & Proctor, R. 2007, *MNRAS*, 377, 759
- Scannapieco, C., Tissera, P. B., White, S. D. M., & Springel, V. 2008, *MNRAS*, 389, 1137

- Schoedel, R., Merritt, D., & Eckart, A. 2009, A&A, in press, arXiv:0902.3892
- Scoville, N. Z., Polletta, M., Ewald, S., Stolovy, S. R., Thompson, R., & Rieke, M. 2001, AJ, 122, 3017
- Semenov, D., Henning, T., Helling, C., Ilgner, M., & Sedlmayr, E. 2003, A&A, 410, 611
- Sersic, J. L. 1968, Atlas de galaxias australes (Cordoba, Argentina: Observatorio Astronomico, 1968)
- Thompson, T. A., Quataert, E., & Murray, N. 2005, ApJ, 630, 167
- van Dokkum, P., et al. 2008, ApJL, 677, L5
- Walcher, C. J., et al. 2005, ApJ, 618, 237
- Walter, F., Riechers, D., Cox, P., Neri, R., Carilli, C., Bertoldi, F., Weiss, A., & Maiolino, R. 2009, Nature, 457, 699
- Weiner, B. J., et al. 2009, ApJ, 692, 187
- Younger, J. D., et al. 2008, ApJ, 688, 59